Dual Environment Effects on the Oxidation of Metallic Interconnects

Gordon R. Holcomb, Malgorzata Ziomek-Moroz, Stephen D. Cramer,
Bernard S. Covino, Jr., and Sophie J. Bullard
Albany Research Center, U. S. Department of Energy
1450 Queen Ave. SW, Albany, OR 97321

Abstract

Metallic interconnects in solid oxide fuel cells are exposed to a dual environment: fuel on one side (i.e. H_2 gas) and oxidizer on the other side (i.e. air). It has been observed that the oxidation behavior of thin stainless steel sheet in air is changed by the presence of H_2 on the other side of the sheet. The resulting dual environment scales are flaky and more friable than the single environment scales. The H_2 disrupts the scale on the air-side. A model to explain some of the effects of a dual environment is presented where hydrogen diffusing through the stainless steel sheet reacts with oxygen diffusing through the scale to form water vapor, which has sufficient vapor pressure to mechanically disrupt the scale. Experiments on preoxidized 316L stainless steel tubing exposed to air/air, H_2/air, and H_2/Ar environments are reported in support of the model.

Introduction

Materials development into producing metallic interconnects for solid oxide fuel cells (SOFC) has many challenges to overcome. One key challenge is that the interconnect must allow the transmission of electrical charge through the interior and through both surfaces. These surfaces are exposed on one side to an oxidizing atmosphere (such as air), and on the other side to a reducing atmosphere for the fuel (such as H_2).

Prior investigations with stainless steels (1-4) have shown that the oxidation behavior, and thus the ability to allow the transmission of electrical charge, is different when exposed to the air-side of a dual environment compared with exposure to a single environment of air. Here a dual environment is defined as exposure of a relatively thin piece of metal to H_2 on one side and to air on the other side.

The observed changes from a single environment to a dual environment include a more porous, flaky, and thicker scale in the dual environment (1-4). One possible explanation for this behavior is that hydrogen diffuses through the metal and changes the point defect chemistry of the oxide, which enhances the diffusion of Cr in chromia scales (2). Another is that the hydrogen that diffuses through the scale reacts with the less stable oxide components of the scale, such as iron oxide (1).

The mechanism proposed here is that hydrogen diffuses through the metal and reacts with oxygen in the scale to form water. As will be shown later, sufficient vapor pressure (steam) may be generated to mechanically form pores in the scale. These pores then allow O_2 to diffuse as a gas through the scale and increase the oxidation rate. The flaky appearance of the scale could be explained by the disruption of the earliest-formed scale by steam pressure.

Some background into the formation of porous scales will be presented, along with calculations of steam pressures. A set of experiments will be presented that aimed to isolate the steam pressure mechanism from other possible hydrogen-scale interactions.

These experiments consisted of exposing preoxidized 316L stainless steel tubes to dual environments of H_2-air and H_2-Ar, and single environments of air-air and Ar-Ar. The lack of O_2 in the H_2-Ar exposure would preclude steam generation as a scale disruption mechanism. The dual environment of H_2-Ar may show, if present, some effects from reactions of hydrogen with the less stable oxides in the scale (1), or with changes in the oxides that form (as compared to the Ar-Ar exposure) that result from increased Cr diffusion (2).

Porous scales

The porous nature of the oxide scale formed in a dual environment can be seen in Fig. 1 for the air-side of 316L exposed to a dual environment of moist H_2-air for 96 hr at 693°C. Figure 1 is a previously unpublished micrograph from Ziomek-Moroz *et al.* (3-4).

This type of porosity is similar to the scales that can form when one of the oxidation products is a gas. One example is the oxidation of HfC, which forms a porous HfO_2 scale and CO gas as reaction products at the carbide-oxide interface (5). The resulting scale is shown in Fig. 2. The partial pressure of CO that forms at the HfC-HfO_2 interface is such that pores form to allow the CO to escape. Subsequently the CO reacts with O_2 from the gas phase to form CO_2 gas. This latter reaction occurs at what is termed the "flame front" within the scale (5). Oxidation rates are much higher for HfC than for Hf because the transport of oxygen can occur though the porous scale.

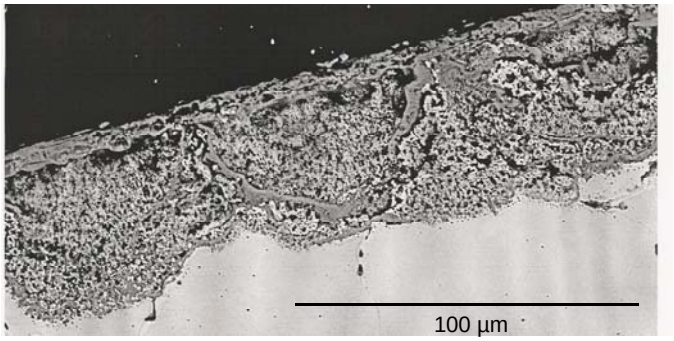

Fig. 1. The porous scale formed on 316L from the air-side of a dual environment exposure of moist H_2-air for 96 hr at 693°C. A previously unpublished micrograph from Ziomek-Moroz *et al.* (3-4).

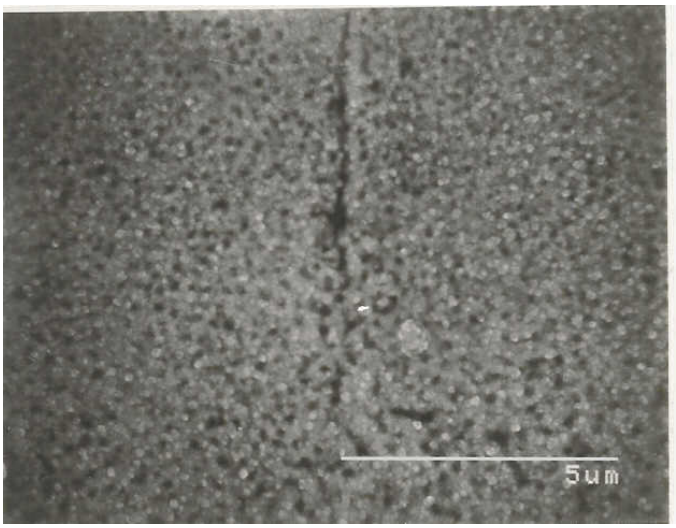

Fig. 2. Cross-section of the porous hafnia scale formed at 1530°C from the oxidation of HfC to HfO_2 and CO_2 (5).

In a similar fashion, pores could be generated in the H_2-air dual environment scale from the formation of steam. The presence of the pores would then allow for rapid oxygen transport through the scale resulting in more oxidation and thicker scales.

Steam formation

The combination of the arrival of hydrogen through the metal and oxygen through the scale can result in a reaction to form water. Water has a very low solubility in the scale, so would be in the form of a gas—steam.

Because chromia is very stable, the partial pressure of water is low at the metal scale interface, as shown in terms of the ratio of P_{H2O}/P_{H2}, Table 1. These calculations are estimates because the hydrogen or oxygen may be in ionic form and the activities of Cr and Cr_2O_3 would not equal 1. The very low P_{H2O}/P_{H2} ratios are nonetheless illustrative that the reaction would not result in large steam pressures at the metal-scale interface.

Table 1. Relative partial pressures for the formation of steam at the metal-scale interface. Based on thermodynamic data from Roine (6), on the reaction $½O_2 + H_2 = H_2O$, and with the activities of Cr and Cr_2O_3 equal to 1.

T, °C	ΔG_f Cr_2O_3 kJ/mol	P_{O2}	ΔG_f H_2O kJ/mol	P_{H2O}/P_{H2}
600	-903	9.6E-37	-200	8.6E-07
700	-878	3.8E-32	-194	5.2E-06
800	-853	2.1E-28	-189	2.2E-05
900	-828	2.7E-25	-187	1.1E-04

However, there would exist a gradient of oxygen pressure or activity from 0.21 in the air to that of the P_{O2} shown in Table 1. Assuming a linear gradient of oxygen partial pressure or activity, and a 1 µm thick scale, a partial pressure of oxygen of 0.0001 would occur approximately 0.5 nm (5Å) from the metal. Using calculations similar to those done for Table 1, and assuming an oxygen partial pressure or activity of 0.0001, the P_{H2O}/P_{H2} ratios are much larger, Table 2. These large ratios suggest high steam pressures sufficient to mechanically alter the scale very near the metal interface. As the scale grows, the scale may sinter, which would result in fewer and larger pores. The image of such a scale would be in agreement with Fig. 1.

Table 2. Relative partial pressures for the formation of steam within the scale near the metal-scale interface. Based on thermodynamic data from Roine (6), on the reaction $½O_2 + H_2 = H_2O$, and with partial pressure or activity of oxygen equal to 0.0001.

T, °C	P_{O2}	ΔG_f H_2O kJ/mol	P_{H2O}/P_{H2}
600	0.0001	-200	8.8E+09
700	0.0001	-194	2.7E+08
800	0.0001	-189	1.5E+07
900	0.0001	-187	2.2E+06

An alternative way to describe the possible steam pressures is with a stability diagram, as shown in Fig. 3. Figure 3 is in terms of log P_{H2} and log P_{O2} for the Cr-O-H and Fe-O-H systems at 700°C. Isobars of P_{H2O}, the diagonal dotted lines, show partial pressures above 1, necessary for void formation, in the upper right-hand part of the diagram. For a P_{O2} of 10^{-4}, a P_{H2} of about 10^{-8} is required for a P_{H2O} of 1.

Experimental procedures

Overall, the experiments consisted of exposing preoxidized 316L stainless steel tubes to dual environments of H_2-air and H_2-Ar, and single environments of air-air and Ar-Ar. Then the resulting scales on the outer diameter of the tubes were examined.

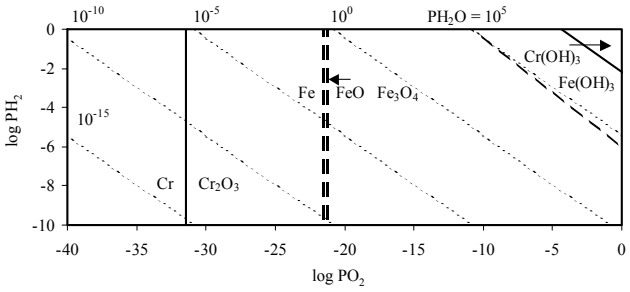

Fig. 3. Phase stability diagram for the Cr-O-H (solid lines) and Fe-O-H (dashed lines) systems at 700°C. Isobars of P_{H2O} are shown as diagonal dotted lines.

The 316L tubes (I.D. 7.76 mm and O.D. 9.32 mm) were preoxidized in dry air at 700°C for 100 hr. Both outside and inside diameters were preoxidized. With the exception of degreasing with methanol, the tubes were exposed in the "as-received" condition.

The preoxidized tubes were then exposed at 700°C for 100 hr in one of four conditions: H_2-air, H_2-Ar, air, and Ar. The dual environment conditions (H_2-air and H_2-Ar) were always with the H_2 in the inside of the 316L tubes. The apparatus for the dual environment experiments is shown in Fig. 4.

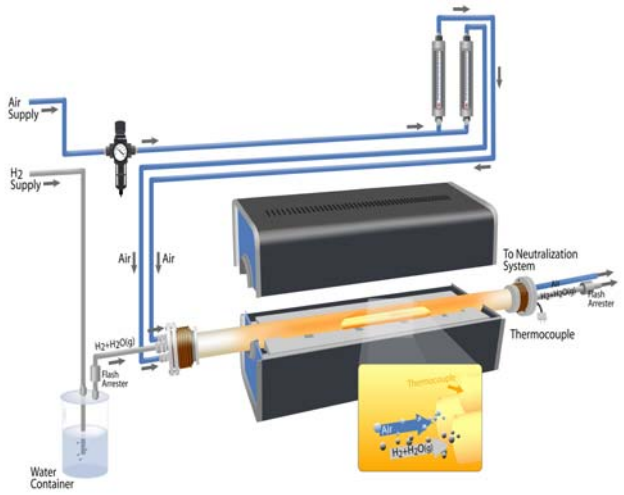

Fig. 4. Dual environment test rig for tubular samples. The current experiments were done with dry H_2 (not bubbled through the water chamber).

The single environment conditions were done during the same furnace runs, but with 3" (7.6 cm) long tube pieces placed inside the furnace chamber. The furnace heat-ups and cool-downs were done at 225°C/hour with a N_2 purge gas. The gas velocity inside the 316L tubes was approximately 430 cm/min. The gas velocity outside the 316L tubes was approximately 5 cm/min.

Post exposure examinations consisted of visual examination of the outside diameter surfaces of the tubes, microscopy (light and scanning electron) of cross-sections, elemental analyses of cross-sections, and x-ray diffraction (XRD) of scales.

Results

Figure 5 shows the outside diameter scales of the tubes. The dual environment effect described earlier (1-4) can be seen by comparing H_2-air with air-air. The H_2-air shows the flaky scale characteristic of dual environments (1-4). There was little difference between the other scales shown in Fig. 5.

Fig. 5. Outer diameter scales after 100 hr exposures at 700°C.

The discontinuous nature of the scale in the H_2-air dual environment scale can be seen in Fig. 6. The inner scale was a Cr-Fe-Ni oxide; the outer scale was Fe_3O_4. The outer scale is the flaky scale seen in the top of Fig. 5.

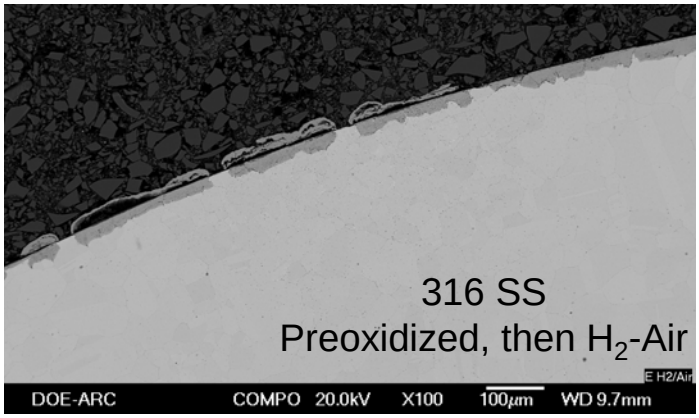

Fig. 6. Backscattered electron image of preoxidized 316L exposed to a dual environment of H_2-air for 100 hr at 700°C. Shown is the outside diameter (the air exposure).

Higher magnification images of each of the exposures are shown in Figs. 7-10. Figure 7 is the H_2-air dual environment near a gap in the scale (as seen in Fig 6). X-ray diffraction and elemental analysis, Table 3, shows the inner scale to be Cr-Fe-Ni oxide with a spinel structure and the outer scale to be Fe_2O_3.

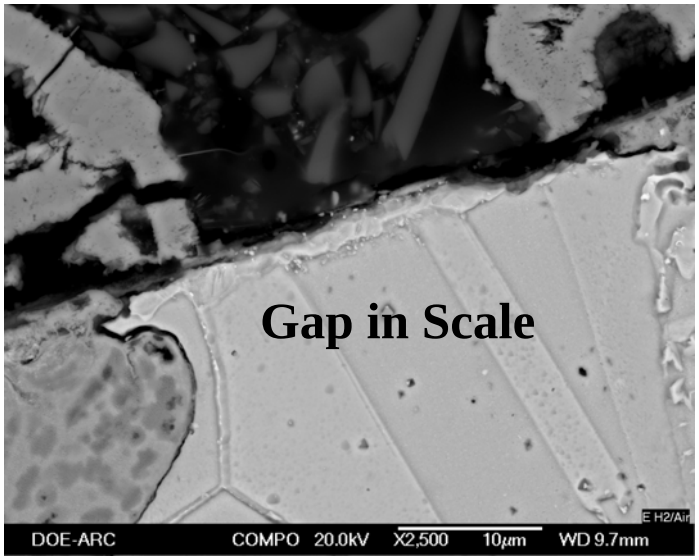

Fig. 7. Backscattered electron image of preoxidized 316L exposed to a dual environment of H_2-air for 100 hr at 700°C. Shown is the outside diameter (the air exposure) at the edge of a gap in the scale (Fig. 6).

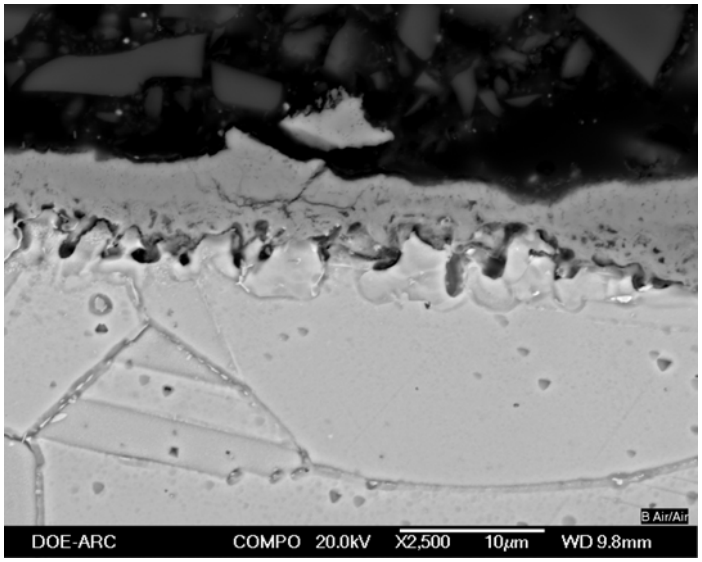

Fig. 8. Backscattered electron image of preoxidized 316L exposed to a single environment of air-air for 100 hr at 700°C. Shown is the outside diameter (the air exposure).

Figure 8 is the air-air single environment. Table 3 shows that the outer part of the scale is Fe oxide. However, the XRD results are more consistent with it being Fe_3O_4. The inner oxide is Cr_2O_3 and a Cr-Fe-Ni spinel. So the scale is much different than in Fig. 7, being much thicker, continuous, and without Fe_2O_3 in the outer oxide.

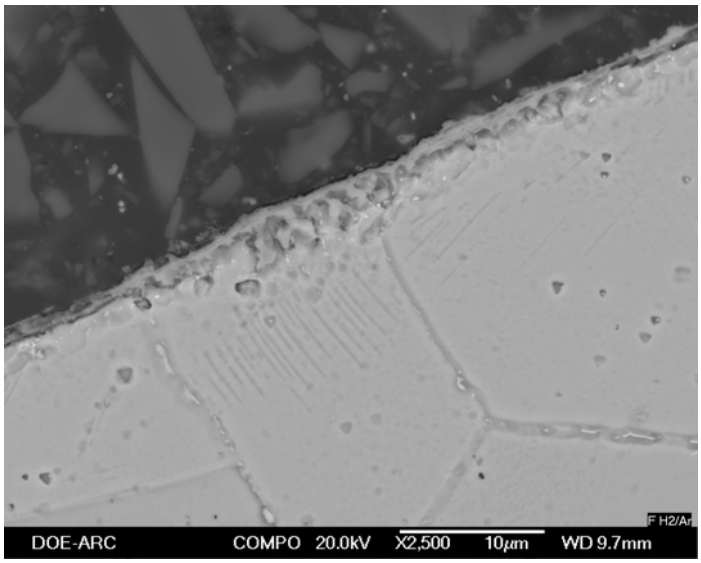

Fig. 9. Backscattered electron image of preoxidized 316L exposed to a dual environment of H_2 Ar for 100 hr at 700°C. Shown is the outside diameter (the air exposure).

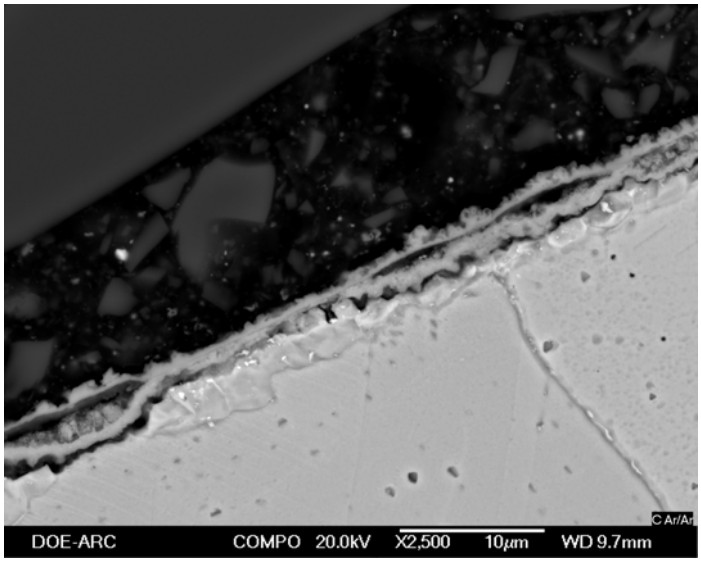

Fig. 10. Backscattered electron image of preoxidized 316L exposed to a single environment of Ar-Ar for 100 hr at 700°C. Shown is the outside diameter (the air exposure).

Figure 9 is the H_2-Ar dual environment. The scale is much different than that found in Figs. 7-8. The scale is much thinner and consists of Cr_2O_3 and a Cr-Fe-Ni spinel (Table 3). The thinness of the scale, as compared with Fig. 8, is not surprising—it was exposed to air at temperature for half of the time.

Figure 10 is the Ar single environment. As in Fig. 9 the scale is Cr_2O_3 and a Cr-Fe-Ni spinel (Table 3). The oxide is partially detached from the metal and in general appears less

protective than in Fig. 8.The separated part of the oxide scale is essentially the same as the attached part of the scale.

Table 3. Results from XRD and elemental analyses for each of the four exposure types. No elemental analyses are given for regions not observed in Figs. 6-10.

		H_2-air	air-air	H_2-Ar	Ar-Ar
Figures		6-7	8	9	10
XRD		$FeCr_2O_4$ Fe_2O_3	$FeCr_2O_4$ Cr_2O_3	$FeCr_2O_4$ Cr_2O_3	$FeCr_2O_4$ Cr_2O_3
Outer	O	57	56		60
Oxide	Fe	42	40		15
Elemental	Cr	0.6	1.8		18
Analysis,	Ni		0.7		0.1
at%	Mo		0.2		0.2
	Mn	0.2	0.9		3
	Si	0.1	0.3		2
Inner	O	50	61	55	60
Oxide	Fe	21	13	17	12
Elemental	Cr	19	20	20	22
Analysis,	Ni	7	3	3	1.4
at%	Mo	1.2	0.7	0.5	0.7
	Mn	1.5	0.5	1.0	1.4
	Si	0.9	1.0	1.9	1.3
Inner	O	51			
Oxide	Fe	19			
Elemental	Cr	21			
Anaylsis	Ni	5			
(Darker	Mo	1.3			
Spots)	Mn	1.6			
at%	Si	1.1			

Discussion

Hydrogen attack of less stable oxides. Examining Figs. 5-8 for dual environment mechanisms, one finds little evidence for hydrogen attack of less stable oxides within the scale (1). If this were the case, then Fig. 7 would show a reaction zone and the scale would probably look less protective than in Fig. 8.

Figure 3 shows that for Cr-O-H and Fe-O-H systems, the formation of $Fe(OH)_3$ and $Cr(OH)_3$ could be possible at very high P_{O2} and P_{H2} conditions. However, XRD results did not find either $Fe(OH)_3$ and $Cr(OH)_3$.

Point defect modification of the scale. The possibility that the dual environment effect is due to protons modifying the oxide to allow for faster Cr or Fe diffusion through the scale (2) is more difficult to examine. This is because a lack of oxygen would also be expected to modify the point defects in the oxide scale.

For chromia scales, Kofstad (7) has used electrical conductivity and diffusion studies to describe the point defect structure in terms of oxygen activity:

The predominant point defects with very low oxygen activity, such as near the Cr-Cr_2O_3 boundary, are chromium interstitials with an effective +3 charge, $Cr_i^{3\cdot}$. Oxygen vacancies, $V_O^{2\cdot}$, with an effective +2 charge may be important minority defects. Under these conditions chromia is a n-type semi-conductor, so the electroneutrality condition (ENC) for chromium interstitials is $3[Cr_i^{3\cdot}] = n$, where n is the concentration of electrons.

At near atmospheric oxygen pressures, the predominant point defects are oxygen interstitials with an effective –2 charge, $O_i^{2'}$, and chromium vacancies with an effective –3 charge, $V_{Cr}^{3'}$. Under these conditions chromia is a p-type semi-conductor, so the ENC for chromium vacancies is $3[V_{Cr}^{3'}] = p$, where p is the concentration of electron holes.

At intermediate oxygen activities stoichiometric defect structures, such as Frenkel ($Cr_i^{3\cdot}$ and $V_{Cr}^{3'}$) or Schottky ($V_{Cr}^{3'}$ and $V_O^{2\cdot}$) defect pairs. The ENC equates the concentration of each defect within the defect pair.

In terms of hydrogen changing the defect structure, the introduced defects could be described either as hydrogen intersitials, $H_i^{\cdot}$, or OH complexes on oxygen sites, $(OH)_O^{\cdot}$. Either case introduces a doping effect with defects having a +1 effective charge. For low oxygen activities, the ENC with doping could become $3[Cr_i^{3\cdot}] + [(OH)_O^{\cdot}] = n$. This would tend to decrease the concentration of chromium interstitials and thus decrease the diffusion of Cr though this part of the scale. Conversely, for high oxygen activities, the ENC could become $3[V_{Cr}^{3'}] = p + [(OH)_O^{\cdot}]$. This would tend to increase the concentration of chromium vacancies and thus increase the diffusion of Cr though this part of the scale.

So for chromia scales, one could conclude that an increase in oxidation rate in dual environments from a modification of the point defect structure increasing the diffusion of chromium could be possible in the outer part of the scale with higher oxygen activities.

But the situation described by point defects is confusing. Kofstad (7) has compared diffusion study results at oxygen activities found at the Cr-Cr_2O_3 interface and has found higher diffusion rates for when oxygen activities were controlled with H_2+H_2O gas mixtures (8) than with CO+CO_2 gas mixtures (9). So a simple doping model, and its effects on the ENC, is not sufficient to describe the situation, even in the relatively simple case of chromia scales—let alone the case of multilayered Cr-Fe oxide scales.

Steam pressure effects. As described earlier under steam formation, H_2O would be expected to form within the scale, albeit close to the metal-scale interface. When oxygen transport is by point defects within the scale, a picture of the activity profiles might look something like Fig. 11. The activity (or partial pressure) of H_2O could be much higher than shown. When the partial pressure of H_2O becomes high enough, pores may form to allow steam to escape, Fig. 12. The pores would also allow oxygen to diffuse into the scale as a gas.

Water formation effects. Besides the physical effects of high steam pressure, simply the presence of water within the scale can change the nature of the oxide scale and the kinetics of scale formation. It is well established that oxidation of steel and stainless steel in moist air, as opposed to dry air, can lead to faster oxidation, less protective scales, and breakaway oxidation (7).

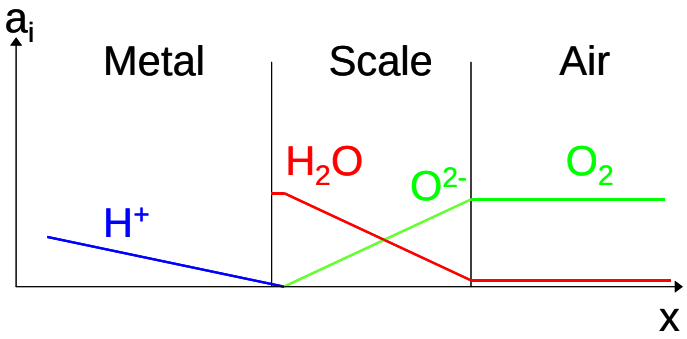

Fig. 11. Schematic of activity profiles during H_2O formation prior to scale disruption. Oxygen transport through the scale is by point defects.

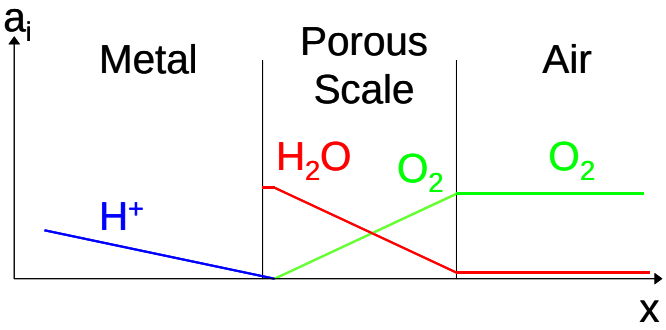

Fig. 12. Schematic of activity profiles during H_2O formation after pore formation. Oxygen transport through the scale is by gaseous diffusion.

Future work

The above experiments and discussion were for 316L in a dual environment. Currently, a dual environment apparatus is being used to test flat samples of more relevant SOFC metallic interconnect alloys. The apparatus is shown in Fig. 13. Alloys being examined include Alloy 230, Crofer 22 APU, J1 and J5. Alloys J1 (Ni-18Mo-12Cr-1.1Ti-0.9Al) and J5 (Ni-22.5Mo-12.5Cr-1Ti-0.1Al-0.5Mn) (10) are nickel based alloys designed for low coefficients of thermal expansion—a useful characteristic for conforming to SOFC seals. Alloy J1 is based on Mitsubishi alloy LTES700 (11).

One difference that can be expected for nickel alloys in dual environments is that there should be less of an effect than for iron alloys. This is because nickel has lower hydrogen permeability than does iron (12). At 700°C, the permeability of hydrogen in pure nickel is about $5x10^{-5}$ cm^2/s; pure iron is about $3x10^{-4}$ cm^2/s (12).

In terms of Fig. 3, if the lower permeability of hydrogen in nickel-base alloys drops the P_{H2} below that required for a P_{H2O} above 1, then sufficient steam pressure would not be expected to form pores.

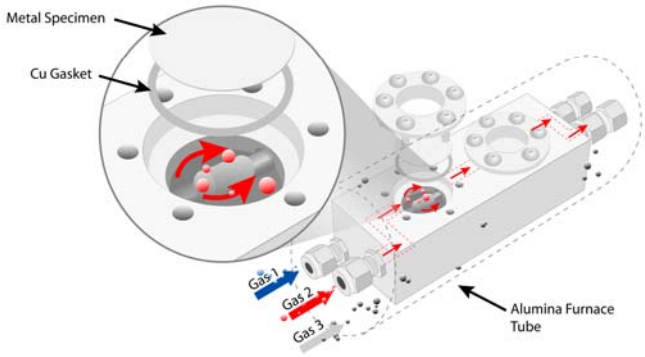

Fig. 13. Apparatus for testing flat samples in a dual environment. The specimen is sealed between the two environments with a copper gasket.

Summary

Dual environments (H_2 on one side and air on the other side) in SOFC systems can degrade the air-side scale compared to that formed in just a single environment of air. The scale becomes thicker, more porous, and tends to delaminate in flakes. All of these differences will degrade the current transfer ability that is required of a SOFC interconnect.

A mechanism to explain some of the effects of a dual environment effect was presented that postulates the reaction of hydrogen (permeated across the metal) with oxygen (diffused though the scale) to form water in the scale very close to the metal interface. The degradation (pores and delamination) of the scale then occurs because of high steam pressure close to the metal-scale interface. The presence of pores allows for faster diffusion of O_2 gas through the scale, resulting in thicker scales.

Experiments were conducted on preoxidized 316L stainless steel tubes in dual environments of H_2-air and H_2-Ar, and single environments of air-air and Ar-Ar. The dual environment effect was present in the H_2-air exposure. No evidence was found for detrimental hydrogen effects in the H_2-Ar dual environment exposure.

References

1. P. Singh and Z. G. Yang, "Thermochemical Analysis of Oxidation and Corrosion Processes in High Temperature Fuel Cells," 131st TMS Annual Meeting, Seattle Washington, Feb 18 (2002)
2. J. W. Stevenson, Z. G. Yang, P. Singh and G. H. Meier, "Corrosion and Corrosion Processes in SOFC Power Generation Systems," 1st International Conference on Fuel Cell Development and Deployment, Storrs, Connecticut, March 9 (2004)
3. M. Ziomek-Moroz, B. S. Covino, Jr., S. D. Cramer, G. R. Holcomb, S. J. Bullard, and P. Singh, "Corrosion of Stainless Steel in Simulated Solid Oxide Fuel Cell Interconnect Environments," paper no 04534 from

Corrosion/2004, NACE International, Houston, Texas (2004)
4. M. Ziomek-Moroz, B. S. Covino, Jr., S. D. Cramer, G. R. Holcomb, S. J. Bullard, P. Singh, and C. F. Windisch, Jr., "Study of Scale Formation on AISI 316L In Simulated Solid Oxide Fuel Cell Bi-Polar Environments," The 29th International Technical Conference on Coal Utilization and Fuel Systems, Clearwater, Florida, April 18-22 (2004)
5. G. R. Holcomb, *The High Temperature Oxidation of Hafnium Carbide*, Ph. D. Thesis, Ohio State University, Columbus, Ohio (1988)
6. A. Roine, *HSC Chemistry 5.11*, Outokumpu Research Oy, Pori, Finland (2002)
7. P. Kofstad, *High Temperature Corrosion*, 116-120, Elsevier Applied Science, New York, New York (1988)
8. L. C. Walters and R. E. Grace, *J. Appl. Phys*., 8, 2331 (1965)
9. K. P. Lillerud and P. Kofstad, *Oxid. Met*., 17, 127-195 (1982)
10. D. E. Alman and P. D. Jablonski, "Low Coefficient of Thermal Expansion (CTE) Nickel Base Superalloys for Interconnect Applications in Intermediate Temperature Solid Oxide Fuel Cells (SOFC)," *Superalloys 2004*, 617-622, TMS, Warrendale, Pennsylvania (2004)
11. R. Yamamoto, Y. Kadoya, H. Kawai, R. Magoshi, T. Noda, S. Hamano, S. Ueta, and S. Isobe, "New Wrought Ni-Based Superalloys with Low Thermal Expansion for 700C Steam Turbines," *Materials of Advanced Power Engineering—2002,* Proc. 7th Liege Conf., Sept 30-Oct 3, 2002, Energy and Technology Vol. 21, Forschungszentium Julich Gmbh Inst. Fur Wekstoffe und Verfahren der Energietechnik (2002)
12. J. Völkl and G. Alefeld, "Diffusion of Hydrogen in Metals," in *Topics in Applied Physics—Hydrogen in Metals I*, 326-329, Springer-Verlag, New York, New York (1978)